

# *Robotic needling system for brachytherapy procedure*

Bardia Konh, Harold Lee, Vincent P. Martin, Vincent Zhao, Parsaoran Hutapea  
Department of Mechanical Engineering  
Temple University  
Philadelphia, USA  
hutapea@temple.edu

**Abstract**—This paper presents a robotic needling system for needle-based percutaneous procedures. This is a novel noninvasive approach being used in many therapeutic surgeries such as brachytherapy where surgeons insert radioactive seeds in a cancerous prostate to kill the unhealthy parts of tissue locally. Studies presented in this work would assist the prediction of bevel-tipped passive needles while being inserted into the patient's body. These needles are deflecting inside the tissue due to the natural viscoelastic resistance of the tissue and the overall reacting forces on the needle's bevel surface. The main aim of this work was to study the effect of having different tip angles at the tip on the final deflection using numerical and experimental methods. This study could be very helpful in path planning and optimizations. Our results showed a higher deflection by a sharper angle at the tip.

**Keywords**—*needle insertion tests, needle-tissue simulation, robotic needling system, interacting forces*

## I. INTRODUCTION

The current trend in today's medical practice aims to minimize invasive procedures of drug delivery, surgeries, etc. One way to do so is to use a flexible needle compared to the traditional rigid needle [1]. Currently, if one were to receive a “shot” from the doctor, a needle would be inserted directly into the desired location and pushed straight through the skin until the tip of the needle has reached the desired area. For areas relatively close to the surface of the skin, the traditional needle suffices. However, if the drug delivery needs to be in a location deep within the body that is surrounded by vital organs, using straight rigid needles or performing surgery on that location would be difficult with straight instruments. Thus, a flexible smart needle would allow for ease of access to these areas. Such a smart needle could be designed by using the actuation forces of shape memory alloy wires as demonstrated in our previous studies [2]. Nitinol is the ideal material for this task [3], because it has super-elastic and a shape memory properties. Its super-elastic property allows this material to bend or stretch greatly before breaking, while its shape memory property allows this material to return to its original shape after bending or stretching. Therefore, by applying Nitinol's properties to create a flexible smart needle [4], a straight path is no longer required for needles, rendering them less invasive for the patients. Currently, the path of the needle arms for this machine are straight and can only be inserted into the patients through straight trajectories. If vital organs are blocking the path, an alternative route must be taken [5]. However, with the flexible smart needle, the needle

arms of the machine can easily avoid the vital organs and go around them [6]. Another application for this type of needle are in medical procedures require precise needle insertions, such as brachytherapy [7]. Brachytherapy is a treatment for patients with prostate cancer that involves the insertion of radioactive seeds within the prostate of the patient. These radioactive seeds emits radiation in small bursts that slowly kills the cancerous cells around it. The normal procedure involves using a straight needle with multiple insertions to place the radioactive seeds. However, using the flexible smart needle, fewer insertions will be required as well as arrange the needle and seeds to be further away from the urethra which is sensitive to radiation. If successful, the Nitinol smart needle would have a major impact in the medical fields. By creating a less invasive needle, the risk of surgeries can be greatly reduced. This is extremely appealing for doctors and surgeons who would seek methods to reduce the risk of injury or death of the patients. In this work the mechanics of a flexible needle inside the body is being discussed while presenting a robotic needling system that is responsible for the surgeon-device communications.

## II. ROBOTIC NEEDELING SYSTEM

### A. Phantom Material as a Substitute for Prostate Tissue

Due to the complexity of nonhomogeneous human tissue and how its mechanical properties can vary based on the location of a specific tissue, the mechanical properties of prostate tissue was chosen as a basis to create the tissue-mimicking phantom. Prostate tissue has been chosen as a reference tissue, because various research has been conducted on prostate tissue to obtain accurate mechanical properties due to the precision of needles required during the surgery. The Modulus of Elasticity of human prostate tissue was approximate  $17.0 \pm 9.0$  kPa based on the studies of [8].

To create the tissue-mimicking test bed, it has been found that a mixture of 3:1 ratio of Plastisol (M-F Manufacturing Co., Ft. Worth, TX, USA) to plastic softener would give a Modulus of Elasticity of approximately 22.29 kPa [9]. To verify this, an indentation test was performed on the test bed to determine its modulus of elasticity [10]. Because the Young's modulus of the test bed is similar to the prostate tissue, it is a good model to test the needle prototype. Alternatively, if other tissue was desired for testing, changing the ratios of Plastisol to softener would alter the mechanical properties of the test bed. Thus, the test bed's elasticity can be

adjusted to mimic the mechanical properties of the various tissues in study.

A liquid Plastisol (PVC) and softener are mixed in a 3:1 ratio, heated to approximately 350°F, and then allowed to cool in to form a gel-like structure. The heating is required, because PVC is a thermoplastic polymer. A mold was created with dimensions of 240x220x30 mm<sup>3</sup>. The mold was constructed with Plexiglas, glued together with Loctite Fast Cure Epoxy, and reinforced with Loctite Silicone Adhesive Sealant. These dimensions was chosen to create a large enough test bed to fit on the experiment apparatus, which will be discussed in more detail in the next section.

### B. Needling Control System: Core and Client Software

Fig. 1 shows the experimental setup [11] used to evaluate the passive needle deflection inside the tissue. The tissue mimicking phantom described in section II.A was used here for needle insertion. A linear motorized stage (Velmex Inc., Bloomfield, NY, USA) of 6µm resolution was used and controlled by the Raspberry Pi system described below. Needle was fixed at one end to the motion controlled and the other end was supported by a guide block close to the tissue. Because of the tiny diameter of the needle and its long length buckling was very probable to happen, especially at initial stages of insertion while tissue was rupturing. An additional support was provided by using a telescope support that kept the outside portion of the needle straight while advancing into the tissue. These needles were inserted into the Plastisol gel with a constant speed of 1.5mm/s by the needle to a motorized linear stage.

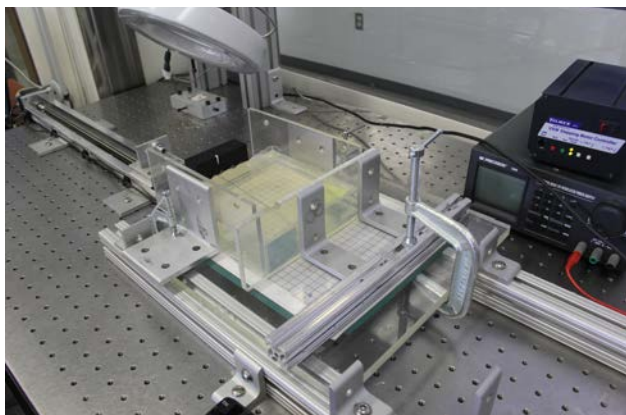


Fig. 1. Experimental needle insertion setup.

The control core was the main point of operation for the control system. Scalability and flexibility could be achieved through the choice of lightweight backend services, hardware platforms and through the use of object oriented server design which allows for multiple instances of power supplies and motor controllers to be used. All communications were handled through this Raspberry Pi (model B from Raspberry Pi Foundation, UK) based server running a custom application, which is written in python. A Raspberry Pi was chosen for the control system due to its small size, low power usage and ability to run the GNU/Linux and the software stack needed to support all operations required from the control system. For example, our current use of the program requires

only one needle, and therefore one power supply and one motor controller. Other versions of this scenario would exist which requires the use of either multiple needles or even a singular needle with a multiple joint requiring multiple power supplies. In this case a power supply could be instantiated for each joint or needle. The block diagram of this system is shown in Fig. 2.

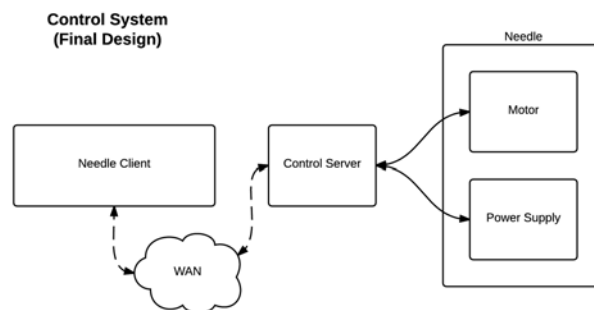


Fig. 2. Block Diagram of Control System and expansion on “Control Server”.

The use of the client/server paradigm in the development of this control system allows for great flexibility. Because of this clients could be written for nearly any computing platform in existence as long as they have the ability to utilize a redis-client library. An android application was developed as a proof of concept. This android application connects to the redis database/control system that was hosted on the Rpi computing platform allowing for the alteration of both the motor controller and the power supply in real time. Fig. 3 shows the two screens that the user interacts with when working with the client application. Note, these screenshots are taken while running on the nexus 7 tablet, but nearly any android device could be used to run this application as long as it has the version 4.4 android and above.

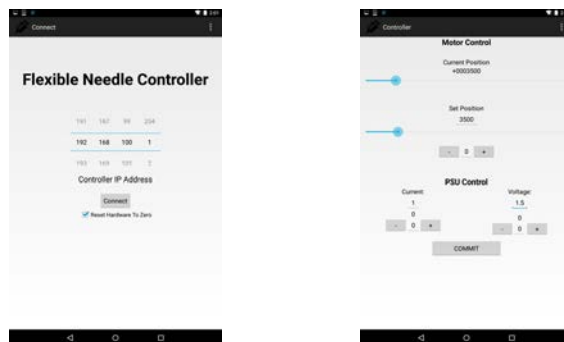


Fig. 3. Login Screen for Android Client.

Because the Raspberry Pi does not come with support for wireless networks, a USB wireless adapter (Wireless Edimax EW-7811Un Adapter) was included to the system. The NAME\_ME\_WIRELESS was selected due to its compatibility with the GNU/Linux operating system. The Raspberry Pi had a limited number of USB ports. In addition it was not supplying enough voltage to power several external devices. Therefore, two USB ports were provided, in addition to a dual analog controller, a wireless network adapter and two USB to RS-232 adapters that were connected and powered.

A GNU/Linux Operating System called Raspbian was chosen because of its ability to support all of the hardware required for this control system. Additionally, the GNU/Linux OS allows for great flexibility in configuration and is open, so software does not need to be purchased. Free, widely used and tested version of the PYTHON programming language, REDIS NOSQL server backend and drivers were all available and their source code viewable in case custom updates must be made. The GNU/Linux operating system also supports the configuration and hosting of a secure wireless network. This allows for client devices to easily attach and use the control system given that they have the proper authentication username and password for the hosted network. Raspbian Linux was the version chosen for this project. This version of Linux was chosen because it supports the Raspberry Pi natively and is Debian based, which allows for easy maintenance of all installed software packages and the installation of any released security updates.

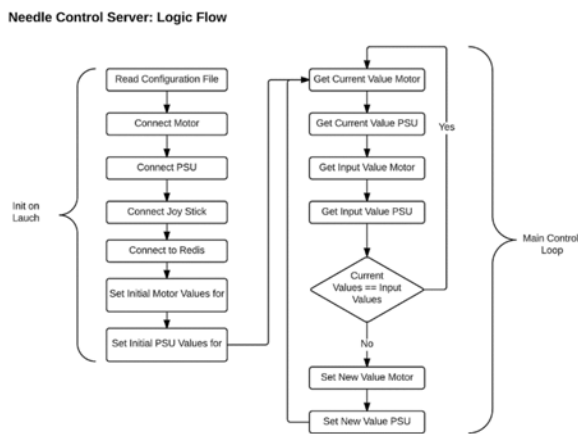


Fig. 4. Needle Control Server Software Flow

Fig. 4 shows the logic flow and how the program will operate from boot up. Initially the program will initialize, read its configuration file. Once this is done it will then have the information needed to connect to the motor controller, power supply and input controller. Once it has these devices it will then attempt to test if they are operational. With the go ahead the program will then set all initial values for the hardware and then enter its control loop and wait for any inputs from either the joystick or the Android application. The insertion of the needle is controlled via a motor controller. The motor controller moves the needle along a track and into the test bed. The motor controller supports RS-232 communication channels and also has full documentation on the methods used to move the motors. This provides a programmer the ability to control the position and speed of the motor. It is through this method that the control server application is able to communicate with the power supply in a manner that allows for needle insertion.

### C. Needle Insertion Simulation

To render the tissue-needle interaction, an appropriate fluid-structure interaction formulation is required as the preparatory step. The major obstacle this simulation faces is the tissue-needle interaction. The solid elements of the needle are carefully considered to penetrate the fluid elements of the

tissue. To study the geometry and mesh of the tissue-needle interaction LS-DYNA (LSTC, Livermore, CA, USA) software was used to generate the model (shown in Fig. 5). A cylinder with a beveled tip was used to model the needle, this increased complexities due to a requirement of a large number of rectangular elements. A rectangular cube was chosen to model the tissue for the overall insertion depth that was desired. For insertion and movement of the needle, a void part was modeled to provide an empty space for a transfer of mass of the tissue. The needle was considered to penetrate and bend inside the tissue at a constant velocity. The Lagrangian Method with a penalty contact algorithm [12] was used to simulate the tissue-needle interaction.

The interaction between the fluid elements of the tissue and the solid elements of the needle utilize the fluid-solid coupling algorithm. The tissue-needle insertion is simulated using the Arbitrary-Lagrangian-Eulerian (ALE) method already available in LS-DYNA. The ALE elements represent the soft tissue. This method, allows for less instability and distortion of the soft tissue elements as a result from the penetration or deformation of the needle. This is due to the nodes, in the ALE type of formulation, which may be rearranged or smoothed to avoid highly twisted and distorted elements. In the ALE method, materials flow through a mesh, which moves itself. On the contrary, due to the flux of material between elements, the governing equations are in more complicated forms. To avoid zero energy modes on elements the hourglass option was used. The manually selected time step was smaller than the particular value predetermined by the software for the defined geometry and material properties. The strain increment was defined as the strain rate times the time step selected. Using this increment, the needle insertion simulations were formed.

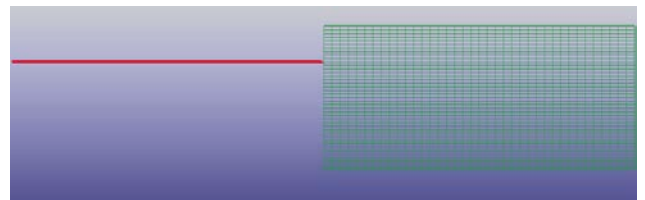


Fig. 5. Needle insertion simulation modeled and analyzed in LSDYNA software.

A 0.64mm diameter, 150mm long needle with a bevel tip angle of 30° was selected to penetrate a tissue modeled as a box of 50x152x4mm<sup>3</sup>. The 8-nodes Solid elements were chosen for both tissue and needle. A void part of the thickness of 1mm was also modeled surrounding the tissue as shown in Fig. 2. The total number of elements of 244, 12464, and 4914 was used in the needle, the tissue, and the void part, respectively. All nodes located on the exterior face of the void part were rigidly constrained. For this model the unit system of Kg-mm-ms was chosen. The needle was inserted from the apex end of the tissue, in the middle of the transverse plane. A motion function with a constant velocity was assigned to the set of nodes located at the ending element of the needle. The prescribed motion curve was defined as a ramp function

varying from zero to 15mm/s in 10s. In order to restrict the translational movement of the tissue in space, all the nodes located on the external boundaries of the void part were constrained to move in x, y and z directions. For the total insertion depth of 150mm, a total simulation time of 10s was required. The results were written to a separate database file in every 0.1s of insertion.

### III. RESULTS

The experimental deflection of the needle is shown in Fig. 6. The needle is inserted into a tissue mimicking phantom. To point out any anomalies and ensure repeatability, the experiment was repeated 5 times per needle at different beveled angles. The deflection of the 0.64mm diameter needle with the bevel-tip angle of 20° is shown in the figure. The deflection of 26.47mm was found while predicted 25.50mm by the LSDYNA model. The results showed an accurate prediction (with only 3.66% error) by the model.

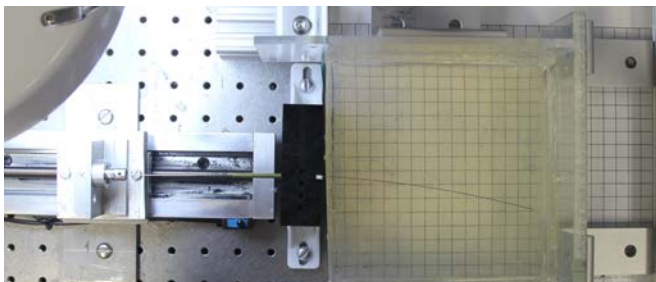


Fig. 6. Deflection of the 0.64mm diameter needle with a bevel-tip angle of 20° into the tissue mimicking phantom.

Fig. 7 shows the averaged needle deflection from the experiment and the simulation. This shows the predicted deflection in comparison to the experimental results. A small difference between predicted deflection and the experimental results was observed. A higher error was found for a higher depth of insertion. This simulation while validated with experiment could to be helpful in optimization, path planning and real time control. Our simulation also provides the capabilities to match with an image-guide control algorithm to improve the outcome of the robotic steering needles inside biological tissues.

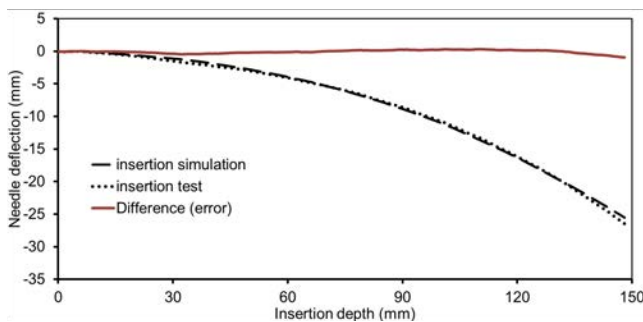


Fig. 7. Comparison between the simulation and experimental results of the 0.64mm diameter needle of bevel-tip angle of 20°. The figure shows the deflection vs. the insertion depth.

Fig. 8 shows the deflection of 0.64mm diameter with different bevel-tip angles into the tissue. It can be seen that for sharp angles (less than 40°), the prediction of the LSDYNA model is

reasonable while the error goes higher for higher angles. While the error is high the difference between the deflections remain lower than 10mm for most of the cases which is considered reasonable for 150mm of insertion depth.

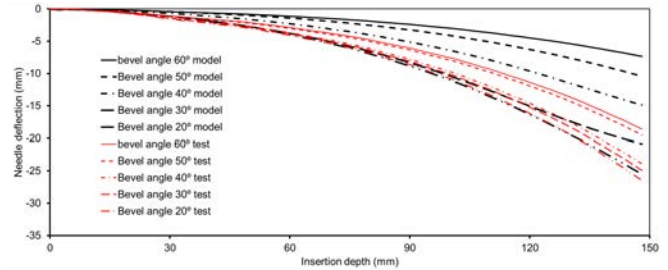


Fig. 8. Comparison between the LSDYNA model and the insertion tests for different needle bevel-tip angles.

Table 1 compares the final needle tip deflections of five different bevel-tip angles for the 0.64mm needle diameter obtained by the needle insertion tests and predicted by LSDYNA model. A smaller deflection was found by having higher angles at the needle's tip. In our simulation, an octagonal prism represented the cylindrical shape of needle with 4 nodes at the cross-section. This meshed shape reduces the interacting bevel area of the needle by 4% compared to the real cylindrical shape. Therefore considering same amount of stress applied to a smaller area, some portion of the error could be explained. Even for the higher error observed in the needle with bevel-tip angle of 60°, the difference of 11.31mm was found which is considered as a good estimation compared to the 150mm of the whole insertion depth. It should be noted that for a short penetration the model is working more accurately while it is mostly the case in surgical procedures.

TABLE 1. Comparison between the deflection of the 0.64mm diameter needle having various bevel-tip angles predicted by the LSDYNA model and the experimental results. The standard deviations were obtained by performing five repetitions of the tests.

Bevel angle	Needle Deflection (mm)		
	LSDYNA model	Insertion test	% error
20	25.50	26.47±0.3	3.66
30	20.80	24.92±0.4	16.53
40	14.80	23.96±0.4	38.23
50	10.40	19.51±1.1	46.69
60	7.30	18.61±0.7	60.77

### IV. DISCUSSION

In this work the deflection of various bevel-tip passive needles is studied inside a tissue mimicking phantom. A robotic needling system has also been introduced that assists the communications between the device and the user. Passive bevel-tip needles are naturally bending inside the tissue due to the interacting forces on their tips. To understand the mechanics of the needle inside the tissue a finite element model was also developed in LSDYNA to predict the total deflection of the needles after 150mm of insertion. The needle-tissue interactions were modeled using Arbitrary-Eulerian-Lagrangian (ALE) formulation. The model could predict the deflection of the needles with reasonable accuracy while the error gets higher for higher tip angles. In our future works we are looking to perform needle insertion tests in ex-vivo tissue and to incorporating non-linear viscoelastic

properties of the tissue in our simulation to find out if the accuracy of the model predictions could be improved.

### Acknowledgment

This work is supported by the Department of Defense CDMRP Prostate Cancer Research Program (GRANT # W81XWH-11-1-0398), and by the graduate school of Temple University.

### References

- [1] T. K. Podder, A. P. Dicker, P. Hutapea, and Y. Yu, "A novel curvilinear approach for prostate seed implantation," *Med. Phys.*, vol. 39, pp. 1887–1892, 2012.
- [2] B. Konh, N. V. Datla, and P. Hutapea, "Feasibility of SMA wire actuation for an active steerable cannula," *J. Med. Device.*, vol. 9, p. 021002, 2015.
- [3] N. V. Datla, M. Honarvar, T. M. Nguyen, B. Konh, K. Darvish, Y. Yu, A. P. Dicker, T. K. Podder, and P. Hutapea, "Towards a nitinol actuator for an active surgical needle," in *ASME Conf. on Smart Material, Adaptive Structures and Intelligent Systems (SMASIS)*, 2012, pp. 265–269.
- [4] B. Konh, M. Honarvar, and P. Hutapea, "Design optimization study of a shape memory alloy active needle for biomedical applications," *Med. Eng. Phys.*, vol. 37, no. 5, pp. 469–477, 2015.
- [5] R. Alterovitz, D. Ritchie, U. C. Berkeley, L. Cho, J. F. O. Brien, K. K. Hauser, K. Goldberg, and J. R. Shewchuk, "Interactive Simulation of Surgical Needle Insertion and Steering," in *Computer Graphics*, 2009, pp. 1–10.
- [6] S. Patil, J. Burgner, R. J. WebsterIII, and R. Alterovitz, "Needle steering in 3-D via rapid replanning," *IEEE Trans. Robot.*, pp. 1–12, 2014.
- [7] T. K. Podder, D. Clark, J. Sherman, D. Fuller, E. Messing, D. Rubens, J. Strang, L. Brasacchio, W. S. N. Liao, and Y. Yu, "In Vivo motion and force measurement of surgical needle intervention during prostate brachytherapy," *Med. Phys.*, vol. 33, no. 8, pp. 2915–2922, 2006.
- [8] B. M. Ahn, J. Kim, L. Ian, K. H. Rha, and H. J. Kim, "Mechanical property characterization of prostate cancer using a minimally motorized indenter in an ex vivo indentation experiment," *Urology*, vol. 76, no. 4, pp. 1007–1011, 2010.
- [9] R. S. Sahebjavaheer, A. Baghani, M. Honarvar, R. Sinkus, and S. E. Salcudean, "Transperineal prostate MR elastography: initial in vivo results," *Magn. Reson. Med.*, vol. 69, no. 2, pp. 411–20, Feb. 2013.
- [10] N. V. Datla, B. Konh, J. Koo, W. C. Daniel, Y. Yu, A. P. Dicker, T. K. Podder, K. Darvish, and P. Hutapea, "Polyacrylamide phantom for self-actuating needle-tissue interaction studies," *Med. Eng. Phys.*, vol. 36, no. 1, pp. 140–145, 2014.
- [11] N. V. Datla, B. Konh, M. Honarvar, T. K. Podder, A. P. Dicker, Y. Yu, and P. Hutapea, "A model to predict deflection of bevel-tipped active needle advancing in soft tissue," *Med. Eng. Phys.*, vol. 36, no. 3, pp. 258–293, 2013.
- [12] *LSTC. LS-DYNA Theory Manual Version 970. r:6030*. Livermore, CA: Livnre Software Technology Corporation (LSTC).